Immunoassay

DOI: 10.1002/anie.200903503

Phospholipid-Coated Carbon Nanotubes as Sensitive Electrochemical Labels with Controlled-Assembly-Mediated Signal Transduction for Magnetic Separation Immunoassay**

*Huagui Nie, Sijia Liu, Ruqin Yu, and Jianhui Jiang**

The increasing interest in proteomics and clinical diagnostics has promoted the development of efficient tools for the sensitive assay of protein biomarkers. The assay is generally performed using certain affinity ligands, such as antibodies and aptamers, that specifically interact with the protein and thus mediate a target-responsive signal transduction cascade. Routine approaches for protein detection include enzyme-linked immunosorbent assays, protein microarrays,[1] magnetic-separation assay,[2] lateral-flow immunoassay,[3] and immunosensors.[4] Electrochemistry holds great potential as the next-generation detection strategy because of its high sensitivity, simple instrumentation, and excellent compatibility with miniaturization technologies. Typically, the performance of electrochemical immunoassay is heavily dependent on the signal-transduction methods. Label-free detection based on electrochemical impedance spectroscopy (EIS)[5] or field-effect transistors (FETs),[6] though being less demanding in terms of operational steps and reagents, have shown limited sensitivity or inadequate resistance to non-specific adsorption. To achieve the enhancement of sensitivity and specificity, a common resort is to exploit signal-transduction labels, such as ligand-conjugated enzymes,[7] or metal-containing nanoparticles.[8] These labels can be transformed into readily detectable electroactive species through enzymatic conversion of certain substrates or chemical decomposition of the metal or its insoluble salts.

Carbon nanotubes (CNTs) exhibit great chemical stability, large aspect ratio, excellent electrical conductivity, and high electrocatalytic activity.[9] These unique properties, coupled with versatile covalent and noncovalent functionalization strategies that are available for conjugation with biological components,[10] make CNTs very promising in the development of high-performance immunosensors for protein detection. Most of CNT-based immunosensors utilize these nanomaterials for the modification of the substrate electrodes.[11] These electrodes, especially the ordered CNT arrays exemplified by single-wall CNT forests,[12] afford efficient platforms for facilitating electron transfer between the electrochemical labels and the electrodes, thus opening up the possibility of sensitivity improvement. An alternative architecture for CNT-based immunosensor is to use semiconducting CNTs configured as FETs.[13] These CNT FET devices can be readily fabricated using a single CNT[13a] or a CNT network[13b] as the electron channel between the source and the drain electrodes. Recent progress in this direction has shown reproducible device characteristics with an immunoassay detection limit in the picomolar range.[13c] Apart from the applications of CNTs in direct electrochemical signal transduction, CNTs can also function as the carriers of conventional electrochemical labels.[14] These CNT-based carriers, though not involved in direct signal transduction, allow the incorporation of numerous electrochemical labels and thus offer the possibility of substantial signal amplification.[14]

Herein we report the proof-of-concept of a novel electrochemical immunoassay strategy based on using phospholipid-coated CNTs as the electrochemical labels. In contrast to conventional electrochemical labels that are immediately converted into electroactive species for electrochemical readouts, the CNT-based labels are controlled assembled on an electrode that is blocked by an insulating self-assembled monolayer (SAM). This CNT assembly then mediates the electrochemistry of certain redox indicators, creating a very sensitive and specific tactic for signal transduction.

The developed electrochemical immunoassay strategy relies on the controlled assembly of multiwalled CNTs (MWNTs) that are specifically collected by a magnetic-separation immunoassay using the phospholipid-coated MWNT labels, as shown in Scheme 1. MWNTs are coated with a mixed SAM of two double-chain phospholipids, phosphocholine (PC) and phosphoethanolamine (PE), through van der Waals and hydrophobic interactions between two phospholipid alkyl chains and the MWNT sidewall.[10a,b] The supramolecular complex of phospholipid-MWNTs not only yields a highly stable suspension in aqueous solution, but ensures the MWNTs are readily conjugated with a monoclonal antibody (MAb_1) through the amine terminals. The resulting MWNT-labeled antibodies can then be exploited, in conjunction with the magnetic beads (MBs) functionalized by another MAb_2, for magnetic-separation-based electrochemical immunoassay. In the assay, the gold electrode is modified with a dense SAM of long-chain alkanethiols, such as 1-octadecanethiol ($C_{18}H_{37}SH$), which isolates the electrode from the aqueous solution with electron transfer between

[*] Dr. H. Nie, Dr. S. Liu, Prof. R. Yu, Prof. Dr. J. Jiang
State Key Laboratory of Chemo/Bio-Sensing and Chemometrics
College of Chemistry and Chemical Engineering
Hunan University, Changsha 410082 (P. R. China)
Fax: (+86) 731-8882-1916
E-mail: jianhuijiang@hnu.cn

[**] This work was supported by "973" National Key Basic Research Program (2007CB310500), NSFC (20875027, 20775023) and NSF of Hunan province (07JJ1002).

Supporting information (experimental details, methods and data) for this article is available on the WWW under http://dx.doi.org/10.1002/anie.200903503.

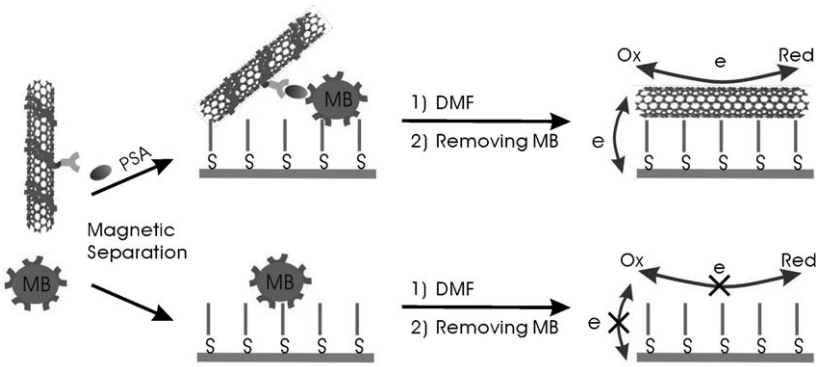

Scheme 1. Electrochemical immunoassay strategy using phospholipid-coated MWNTs as electrochemical labels. In the presence of an antigen protein (PSA), magnetic separation collects the immunocomplex formed between MWNT-labeled MAb_1 and magnetic-bead (MB) modified MAb_2 on an isolating SAM-modified electrode. Treatment with DMF dissociates the phospholipid from the MWNTs, leaving the MWNTs assembled on the SAM. With the MBs removed by a magnet, the assembled MWNTs mediate electron transfer between electroactive species and the electrode, triggering the electrochemical signal. Bottom: In the absence of antigen (PSA) there is collection of the labels by magnetic separation, thus no MWNTs assemble on the isolating SAM and no current signal obtained.

redox solutes and the electrode obstructed. In the presence of the protein antigens (PSA), an immunocomplex, sandwiching the antigen protein, is formed between the MWNT-labeled MAb_1 and the magnetic-bead-modified MAb_2. The immunocomplex can be collected using an external magnetic field and transported on the $C_{18}H_{37}SH$-blocked electrode surface. On addition of *N*,*N*-dimethylformamide (DMF) to the immunocomplex suspension on the electrode surface, the phospholipid coatings on the MWNTs are dissolved in the organic solvent, inducing the MWNT labels to be released from the immunocomplexes. This process results in the MWNTs being precipitated from the solution and assembled on the $C_{18}H_{37}SH$-blocked electrode surface by van der Waals and hydrophobic interactions between the long alkyl chains and the MWNT sidewall.[15] With the magnetic beads removed by a magnet to eliminate possible nonspecific adsorption, the MWNTs adsorbed on the isolating $C_{18}H_{37}SH$ SAM mediate efficient electron transfer between the electrode and an electroactive species, such as ferrocenecarboxylic acid (FcCOOH). This results in a strong redox current dependent upon the surface area of the MWNTs adsorbed on the $C_{18}H_{37}SH$ SAM. In the absence of the antigen, no MWNT-labels are collected in the magnetic separation and so no MWNTs can be released and assembled on the isolating SAM after the DMF treatment. In this case, when the magnetic beads are removed by a magnet, the isolating property of the SAM is not altered and no remarkable current signal is obtained. Note that in the assay, a single MWNT label can mediate the redox response of numerous FcCOOH molecules, implying that the MWNT-based label system indeed offers a highly efficient signal amplification in electrochemical transduction. Moreover, as more antigens are expected to cause in more MWNTs to assemble on the $C_{18}H_{37}SH$ SAM the current responses offers a quantitative measure for the antigen concentration. It is also noteworthy that this strategy not only utilizes the electron-conducting properties of MWNTs, but also combines some unique properties of MWNTs including noncovalent modification of phospholipids for biomolecular conjugation, dissociation of phospholipid coating from MWNT surface by DMF, and selective assembly of bare MWNTs on hydrophobic SAM. Gold nanoparticles do not have these properties, so can not be used in this immunoassay.

The immunoassay strategy was tested using a model target of prostate specific antigen (PSA), a highly selective protein biomarker associated with tumors.[16] Figure 1 shows typical cyclic voltammogram (CV) responses using the developed technique. With the electrode modified by the $C_{18}H_{37}SH$ SAM, there were no appreciable current peaks in the CV curves, suggesting that the $C_{18}H_{37}SH$ SAM formed a fully isolating layer and the electron transfer between the redox indicator FcCOOH and the electrode was almost completely blocked.

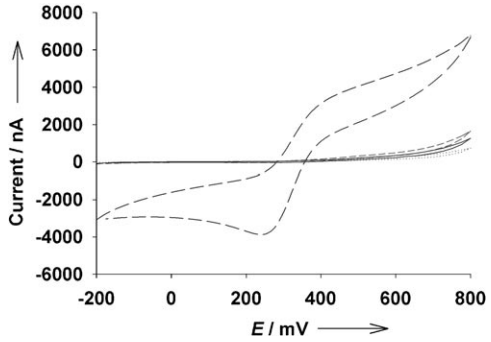

Figure 1. Cyclic voltammograms obtained for the $C_{18}H_{37}SH$-blocked electrode (•••••), the immunoassay of 100 ng mL^{-1} PSA with MWNT labels (– – –), the immunoassay of 100 ng mL^{-1} PSA with liposome labels (——), and the immunoassay of 1 μg mL^{-1} BSA with MWNT labels (-----). Scan rate is 100 mV s^{-1}. All potentials are referenced to the SCE. Measurements were performed in 20 mM phosphate buffer (pH 7.4) containing 0.1 M $KClO_4$ and 5 mM FcCOOH.

In the presence of PSA protein (100 ng mL^{-1}), a pair of obvious current peaks appeared at 250 mV and 350 mV versus saturated calomel electrode (SCE), a typical redox peak range of ferrocene derivatives. A control experiment was performed using liposome-labeled MAb_1 in place of the MWNT-tagged MAb_1 in the immunoassay. The control gave no significant redox peaks in the CV. Combining these two observations shows that the current peaks in the assay arise from the MWNT labels, implying that the MWNT labels alter the isolating properties of the $C_{18}H_{37}SH$ SAM and mediate the redox of FcCOOH at the electrode surface. A further control experiment used another protein target, 1 μg mL^{-1} bovine serum albumin (BSA), instead of PSA, and no visible current peaks in the CV. This result shows that the MWNT labels could only be collected as immunocomplexes sand-

wiching the PSA targets. Thus the phospholipid-coated MWNTs afforded specific labels for electrochemical immunoassay.

Differential pulse voltammograms (DPVs; see Figure S1a in the Supporting Information) showed only a very small peak, approximately 21 nA (with a standard deviation (SD) of 6.7% across five repetitive measurements) for the $C_{18}H_{37}SH$-blocked electrode. The MWNT-labeled MAb_1, in the presence of 100 ng mL^{-1} PSA yielded a strong DPV signal, 1386 nA (SD of 4.1% across five repetitive measurements). In contrast, no significant DPV peak (ca. 36 nA, SD of 5.6% across five repetitive measurements) was obtained in the control experiment where the MWNT-labeled MAb_1 was replaced by the liposome-tagged MAb_1, even in the presence of 100 ng mL^{-1} PSA target. Also, the blank experiment with 100 ng mL^{-1} PSA replaced by 1 μg mL^{-1} BSA gave an insignificant DPV peak (ca. 45 nA, SD of 5.9% across five repetitive measurements) even with the MWNT-labeled MAb_1. For the DPV response to 100 ng mL^{-1} PSA, an extremely desirable signal-to-background ratio of approximately 31 was readily acquired, which indicates a high dose-response sensitivity of the strategy. Additional control experiments were also conducted with other proteins or matrices, such as human immunoglobulins G (IgG), carcinoembryonic antigen (CEA), α-fetoprotein (AFP), carbohydrate antigen (CA) 19-9, CA 125, CA 15-3, transferrin (TF), human serum albumin (HSA), and bovine serum (Figure S1b in the Supporting Information). The results revealed that none of these protein targets produced a substantial DPV response in the assay using MWNT-labeled MAb_1. These DPV observations confirmed that the DPV signals arising from the MWNT labels collected in magnetic separation, and the strategy was very sensitive and specific for the detection of PSA.

The key hypothesis of the signal-transduction mechanism is that the assembly of MWNTs on the isolating $C_{18}H_{37}SH$ SAM could mediate efficient electrochemistry of redox species, and that treatment with DMF did not alter the isolating properties of the SAM. A control experiment, in which bare MWNTs were assembled on the SAM-modified electrode, was performed (Figure S2 in the Supporting Information). Both the CV and DPV responses showed large redox peaks arising from FcCOOH, confirming that MWNT assembly on the $C_{18}H_{37}SH$ SAM mediated efficient redox of the electroactive species. Also, DMF treated SAM-modified electrodes were investigated electrochemically and by scanning electron microscopy (SEM) techniques (Figure S2 and S3 in the Supporting Information) which also verified that this treatment had little effect on the isolating SAM layer.

After the magnetic separation, transmission electron microscopy (TEM) investigation of the collected immunocomplexes showed that the presence of 100 ng mL^{-1} PSA resulted in an agglutinated complex of magnetic beads and MWNTs, while clearly separated magnetic beads with no MWNT aggregates were obtained for the blank sample with 1 μg mL^{-1} BSA (Figure S4 in the Supporting Information), confirming that the MWNT labels could only be collected by the magnetic separation with the PSA-sandwiched immunocomplexes.

The immunocomplexes deposited on the electrode were studied by SEM (Figure 2). For the blank sample with 1 μg mL^{-1} BSA, close-heaped magnetic beads were observed on the surface. After the DMF treatment and collection of magnetic beads using a magnet, most of the magnetic beads were removed. In contrast, the immunocomplexes collected in magnetic separation assay of 100 ng mL^{-1} PSA yielded a tangled agglomerate of magnetic beads and MWNTs. Interestingly, after the DMF treatment and the magnetic removal of the beads, a pile of large MWNT aggregates together with a few beads was observed adsorbed on the surface, implying that the DMF treatment dissociates the MWNTs from the immunocomplexes and the beads could be removed without substantial loss of MWNTs. Note that large MWNT aggregates on the surface could also mediate electron transfer through the connected MWNT networks, hence the aggregation of MWNTs would not affect the signal transduction.

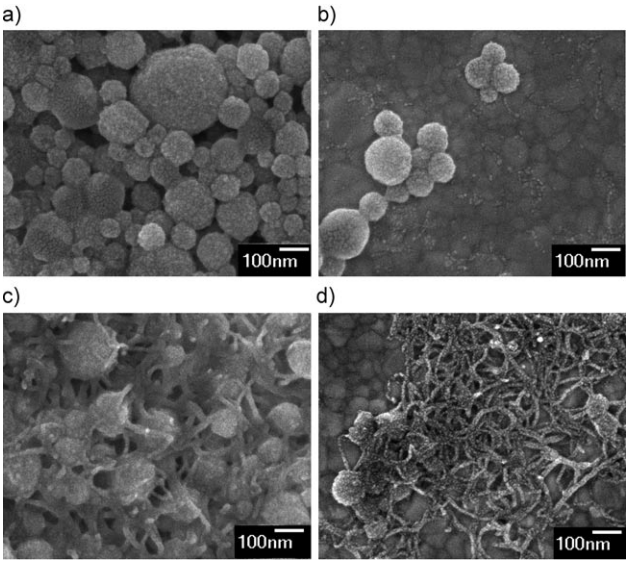

Figure 2. SEM images of a) the immunocomplexes with 1 μg mL^{-1} of BSA, deposited on the electrode after collection by magnetic separation, b) after treatment with DMF and magnetic removal of magnetic beads. SEM images of c) the immunocomplexes for 100 ng mL^{-1} PSA collected by magnetic separation, d) after treatment with DMF and magnetic removal of magnetic beads.

Electrochemical impedance spectroscopy (EIS; see Figure S5 in the Supporting Information) shows that the $C_{18}H_{37}SH$-blocked electrode gave a very large impedance, indicating the isolating behavior of the $C_{18}H_{37}SH$ SAM. The complexes collected for the blank sample showed a decreased impedance response. After DMF treatment and removal of the magnetic beads, the impedance increased suggesting that magnetic beads deposited on the surface could change the isolating property of the $C_{18}H_{37}SH$ SAM, and the removal of the beads would minimize the background signal. In contrast, the immunocomplexes collected for the PSA sample had a much smaller impedance than that of the blank sample, and the impedance decreased slightly after DMF treatment and magnetic-bead removal.

Considering the poor conductivity of magnetic beads, the selective removal of beads, while the highly conductive MWNTs are retained on the $C_{18}H_{37}SH$-blocked electrode surface, was expected to improve the performance in electrochemical signal transduction (Figure S6 in the Supporting Information). After DMF treatment and bead removal, a strong DPV signal (ca. 1351 nA) was achieved for the PSA sample with a very low background current (ca. 45 nA) arising from the blank sample, affording very desirable assay performance. However, DMF treatment before the beads are removed, gives a stronger DPV signal (ca. 1585 nA) together with an increasing background response (ca. 82 nA), revealing that the adsorption of magnetic beads on the $C_{18}H_{37}SH$-blocked electrode could alter the isolating properties of the SAM. Thus the selective removal of the beads from the electrode surface could substantially improve the signal-to-noise ratio. In cases where the immunocomplexes were not treated by DMF, the DPV responses were much smaller than those acquired after DMF treatment. This might be because the phospholipid coatings on the MWNTs hinder the electron transfer between the MWNTs and the electrode. In this case, the DPV signal became very low if the magnetic beads were removed, indicating that the removal of the beads without DMF treatment would induce substantial loss of the MWNT labels. These observations confirmed that the DMF treatment of the immunocomplexes plays a crucial role in the electrochemical transduction.

When DMF was added into an aliquot of the MWNT-labeled antibody solution, MWNT aggregates formed immediately, and four hours later almost all the MWNTs had precipitated giving a transparent supernatant solution (Figure S7 in the Supporting Information) and confirming that the MWNT labels could dissociated from the immunocomplexes under the DMF treatment.

Figure 3 shows typical DPV curves obtained in response to varying PSA concentrations. There is a nonlinear increase in DPV response with increasing PSA concentrations ($0\,pg\,mL^{-1}$ to $100\,ng\,mL^{-1}$). This nonlinear response results from the limited amounts of antibody-modified magnetic beads and MWNT labels, which mean that at high PSA concentrations the equilibrium of the immuno-reaction is dependent on the concentrations of magnetic beads and MWNTs. Saturate current responses were found at high PSA concentrations over $50\,ng\,mL^{-1}$, which is attributed to the limited amount of beads available for collecting MWNT labels and the limited thickness of the MWNT aggregates that can be stably adsorbed on the electrode surface. A quasi-linear response was obtained in a logarithmic concentration scale within a four-order of magnitude concentration range from $5\,pg\,mL^{-1}$ to $50\,ng\,mL^{-1}$ with a readily achieved detection limit of $3\,pg\,mL^{-1}$ (Figure S8 in the Supporting Information). In addition to the substantially improved signal gain of approximately 30, this technique also gave a detection sensitivity among the best in CNT-based immunoassays.[3a,6b,13c] Note the potential shift in the DPV curves to more negative values at higher PSA concentrations. At higher PSA concentrations there are more MWNT aggregates on the $C_{18}H_{37}SH$ SAM giving a bigger electron-conducting network. The efficiency of electron-tunneling between the electrode and the MWNT network thus increases, allowing faster electron transfer between the electrode and the redox species.

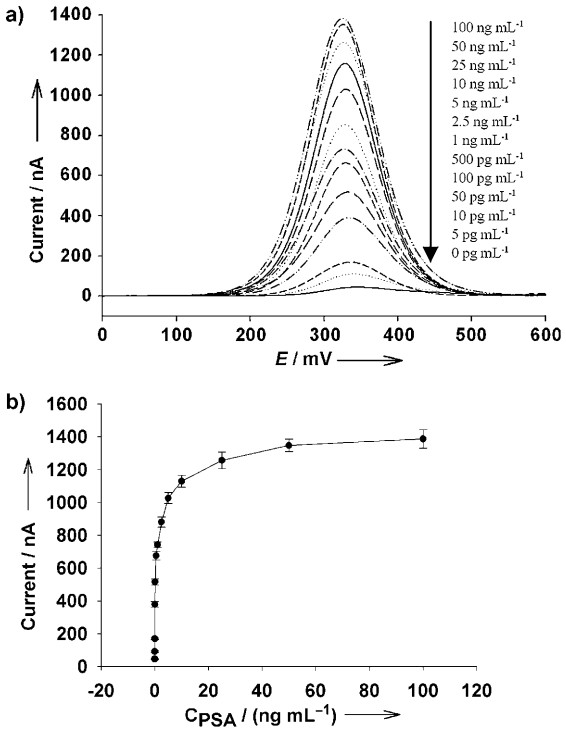

Figure 3. a) Typical DPV response curves for different PSA concentrations. b) DPV peak currents for different PSA concentrations. Potential scanning was from 600 to 0 mV at $10\,mV\,s^{-1}$ with an amplitude of 25 mV. All potentials are referenced to SCE. Measurements were performed in 20 mM phosphate buffer (pH 7.4) containing 0.1 M $KClO_4$ and 5 mM FcCOOH.

The technique was further validated by using 15 clinical serum specimens with reference to a commercialized chemiluminescence immunoassay (CLIA) method. The estimated concentrations of PSA in these samples using our technique showed deviations ranging from 4.36% to 15.69% from those obtained using CLIA (Figure S9 in the Supporting Information). These results demonstrated that our strategy provided assay performance comparable to the commonly used method, and might hold promise as a viable technique for the determination of PSA in serum samples.

In conclusion, we developed a novel electrochemical immunoassay strategy based on using phospholipid-coated MWNTs as the electrochemical labels. These electrochemical labels could be easily prepared by the noncovalent modification of the MWNTs and covalent conjugation with antibodies. Also, these labels could be readily incorporated into a magnetic-separation-based immunoassay. Because magnetic separation allows highly effective and selective accumulation of the electrochemical labels and the assembly of a single MWNT label mediated the redox response of numerous indicator molecules, this strategy could afford improved sensitivity and specificity in signal transduction over conventional techniques. The strategy was demonstrated to exhibit dynamic responses to the protein target over a four order-of-magnitude concentration range with a desirably high signal gain and low detection limit. Since magnetic separation

allowed parallel collection of multiple protein targets, this strategy could also be implemented for simultaneous detection of numerous proteins or samples using a densely packed sensing array format. In view of these advantages, this new electrochemical immunoassay strategy is has potential for point-of-care applications in proteomic research and clinical diagnostics.

Received: June 29, 2009
Revised: August 25, 2009
Published online: November 24, 2009

Keywords: carbon nanotubes · controlled assembly · electrochemistry · immunoassays · phospholipids

[1] a) D. S. Wilson, S. Nock, *Angew. Chem.* **2003**, *115*, 510 – 517; *Angew. Chem. Int. Ed.* **2003**, *42*, 494 – 500; b) Z. Chen, S. M. Tabakman, A. P. Goodwin, M. G. Kattah, D. Daranciang, X. R. Wang, G. Y. Zhang, X. L. Li, Z. Liu, P. J. Utz, K. L. Jiang, S. S. Fan, H. J. Dai, *Nat. Biotechnol.* **2008**, *26*, 1285 – 1292.

[2] L. Z. Gao, J. Zhuang, L. Nie, J. B. Zhang, Y. Zhang, N. Gu, T. H. Wang, J. Feng, D. L. Yang, S. Perrett, X. Y. Yan, *Nat. Nanotechnol.* **2007**, *2*, 577 – 583.

[3] a) G. D. Liu, Y. Y. Lin, J. Wang, H. Wu, C. M. Wai, Y. H. Lin, *Anal. Chem.* **2007**, *79*, 7644 – 7653; b) N. A. Shaikh, J. Ge, Y. X. Zhao, P. Walker, M. Drebot, *Clin. Chem.* **2007**, *53*, 2031 – 2034.

[4] a) S. M. Borisov, O. S. Wolfbeis, *Chem. Rev.* **2008**, *108*, 423 – 461; b) N. Backmann, C. Zahnd, F. Huber, A. Bietsch, A. Pluckthun, H. P. Lang, H. J. Guntherodt, M. Hegner, C. Gerber, *Proc. Natl. Acad. Sci. USA* **2005**, *102*, 14587 – 14592.

[5] G. Tsekenis, G. Z. Garifallou, F. Davis, P. A. Millner, T. D. Gibson, S. P. J. Higson, *Anal. Chem.* **2008**, *80*, 2058 – 2062.

[6] a) Y. Cui, Q. Q. Wei, H. Park, C. M. Lieber, *Science* **2001**, *293*, 1289 – 1292; b) M. Briman, E. Artukovic, L. Zhang, D. Chia, L. Goodglick, G. Gruner, *Small* **2007**, *3*, 758 – 762.

[7] a) D. P. Tang, J. J. Ren, *Anal. Chem.* **2008**, *80*, 8064 – 8070; b) M. S. Wilson, W. Y. Nie, *Anal. Chem.* **2006**, *78*, 6476 – 6483.

[8] a) J. A. Ho, Y. C. Lin, L. S. Wang, K. C. Hwang, P. T. Chou, *Anal. Chem.* **2009**, *81*, 1340 – 1346; b) K. Y. Chumbimuni-Torres, Z. Dai, N. Rubinova, Y. Xiang, E. Pretsch, J. Wang, E. Bakker, *J. Am. Chem. Soc.* **2006**, *128*, 13676 – 13677.

[9] a) S. N. Kim, J. F. Rusling, F. Papadimitrakopoulos, *Adv. Mater.* **2007**, *19*, 3214 – 3228; b) M. Pumera, *Chem. Eur. J.* **2009**, *15*, 4970 – 4978.

[10] a) N. W. S. Kam, Z. Liu, H. J. Dai, *J. Am. Chem. Soc.* **2005**, *127*, 12492 – 12493; b) C. Richard, F. Balavoine, P. Schultz, T. W. Ebbesen, C. Mioskowski, *Science* **2003**, *300*, 775 – 778; c) S. S. Wong, E. Joselevich, A. T. Woolley, C. L. Cheung, C. M. Lieber, *Nature* **1998**, *394*, 52 – 55.

[11] a) R. L. McCreery, *Chem. Rev.* **2008**, *108*, 2646 – 2687; b) S. Viswanathan, L. C. Wu, M. R. Huang, J. A. Ho, *Anal. Chem.* **2006**, *78*, 1115 – 1121; c) K. Gong, S. Chakrabarti, L. M. Dai, *Angew. Chem.* **2008**, *120*, 5526 – 5530; *Angew. Chem. Int. Ed.* **2008**, *47*, 5446 – 5450; d) A. Merkoci, M. Pumera, X. Llopis, B. Perez, M. D. Valle, S. Alegret, *TrAC Trends Anal. Chem.* **2005**, *24*, 826 – 838.

[12] a) J. J. Gooding, R. Wibowo, J. Q. Liu, W. R. Yang, D. Losic, S. Orbons, F. J. Mearns, J. G. Shapter, D. B. Hibbert, *J. Am. Chem. Soc.* **2003**, *125*, 9006 – 9007; b) F. Patolsky, Y. Weizmann, I. Willner, *Angew. Chem.* **2004**, *116*, 2165 – 2169; *Angew. Chem. Int. Ed.* **2004**, *43*, 2113 – 2117.

[13] a) A. Star, J. P. Gabriel, K. Bradley, G. Gruner, *Nano. Lett.* **2003**, *3*, 459 – 463; b) H. R. Byon, H. C. Choil, *J. Am. Chem. Soc.* **2006**, *128*, 2188 – 2189; c) B. L. Allen, P. D. Kichambare, A. Star, *Adv. Mater.* **2007**, *19*, 1439 – 1451.

[14] a) J. Wang, G. D. Liu, M. R. Jan, *J. Am. Chem. Soc.* **2004**, *126*, 3010 – 3011; b) X. Yu, B. Munge, V. Patel, G. Jensen, A. Bhirde, J. D. Gong, S. N. Kim, J. Gillespie, J. S. Gutkind, F. Papadimitrakopoulos, J. F. Rusling, *J. Am. Chem. Soc.* **2006**, *128*, 11199 – 11205.

[15] a) Y. H. Wang, D. Maspoch, S. L. Zou, G. C. Schatz, R. E. Smalley, C. A. Mirkin, *Proc. Natl. Acad. Sci. USA* **2006**, *103*, 2026 – 2031; b) L. Su, F. Gao, L. Q. Mao, *Anal. Chem.* **2006**, *78*, 2651 – 2657.

[16] Y. Huang, T. H. Wang, J. H. Jiang, G. L. Shen, R. Q. Yu, *Clin. Chem.* **2009**, *55*, 964 – 971.

